NANO LETTERS

Letter

pubs.acs.org/NanoLett

Influence of Size-Induced Oxidation State of Platinum Nanoparticles on Selectivity and Activity in Catalytic Methanol Oxidation in the Gas Phase

Hailiang Wang, Yihai Wang, Zhongwei Zhu, Andras Sapi, Kwangjin An, Griffin Kennedy, William D. Michalak, and Gabor A. Somorjai*

Department of Chemistry, University of California, Berkeley, California 94720, United States, and Materials Sciences and Chemical Sciences Divisions, Lawrence Berkeley National Laboratory, Berkeley, California 94720, United States

Supporting Information

ABSTRACT: Pt nanoparticles with various sizes of 1, 2, 4, and 6 nm were synthesized and studied as catalysts for gas-phase methanol oxidation reaction toward formaldehyde and carbon dioxide under ambient pressure (10 Torr of methanol, 50 Torr of oxygen, and 710 Torr of helium) at a low temperature of 60 °C. While the 2, 4, and 6 nm nanoparticles exhibited similar catalytic activity and selectivity, the 1 nm nanoparticles showed a significantly higher selectivity toward partial oxidation of methanol to formaldehyde, but a lower total turnover frequency. The observed size effect in catalysis was correlated to the size-dependent structure and oxidation state of the Pt nanoparticles. X-ray photoelectron spectroscopy and infrared vibrational spectroscopy using adsorbed CO as molecular probes revealed that the 1 nm nanoparticles were predominantly oxidized while the 2, 4, and 6 nm nanoparticles were largely metallic. Transmission electron microscopy imaging witnessed the transition from crystalline to quasicrystalline structure as the size of the Pt nanoparticles was reduced to 1 nm. The results highlighted the important impact of size-induced oxidation state of Pt nanoparticles on catalytic selectivity as well as activity in gas-phase methanol oxidation reactions.

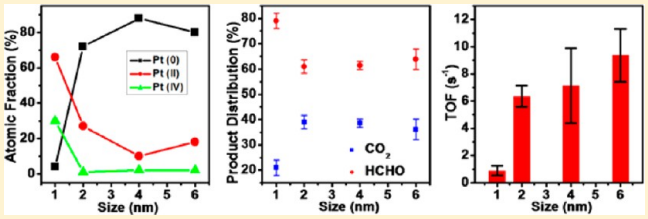

KEYWORDS: *Heterogeneous catalysis, methanol oxidation, Pt nanoparticles, size effect*

The effect of nanoparticle size on catalytic performance is an important topic in heterogeneous catalysis.[1−9] Enabled by the evolution of colloidal synthesis, Pt nanoparticles with controlled size distributions have been successfully prepared and used to understand how catalytic performance changes with nanoparticle size for various chemical reactions.[10] Pt nanoparticles with different sizes exhibited significantly different catalytic selectivity and activity for structurally sensitive reactions including methylcyclopentane/hexane reformation,[4,5] crotonaldehyde hydrogenation,[6] cyclohexene hydrogenation/dehydrogenation,[7] pyrrole hydrogenation,[8] benzene/toluene hydrogenation,[11] and 1,3-butadiene hydrogenation.[12] Such size effects are often observed in the size range of ∼1−7 nm, where the percentage of step/edge atoms changes drastically.[4,13]

Importantly, theoretical simulation has suggested that chemical and electronic structures of Pt nanoparticles below a certain size could be substantially different from those of metallic solids as most of the atoms become oxidized.[14,15] However, it still remains challenging to identify such structural transitions experimentally. It is also elusive how such transitions may affect the catalytic properties of Pt nanoparticles.

Selective oxidation of alcohols is an important transformation process in energy conversion and chemical synthesis. Methanol is the fuel for direct methanol fuel cells in which full oxidation of methanol at low overpotential is desirable to maximize the energy production.[16] In addition, partial oxidation of methanol by molecular oxygen at low temperature is an efficient and environmentally benign way of producing valuable chemicals such as formaldehyde and formic acid.[17] Therefore, it is highly important to explore the structure−property relationship of Pt nanoparticles in the selective oxidation of methanol.

In this work, we investigated Pt nanoparticles with various sizes (1, 2, 4, and 6 nm, respectively) as catalysts for gas-phase methanol oxidation reactions under ambient pressure (10 Torr of methanol, 50 Torr of oxygen, and 710 Torr of helium) at 60 °C. We found Pt nanoparticles with sizes of 2, 4, and 6 nm simultaneously produced ∼60% of formaldehyde and ∼40% of carbon dioxide in the oxidation process, which was independent of the partial pressure of oxygen. Interestingly, 1 nm Pt nanoparticles showed significantly higher selectivity toward partial oxidation of methanol to formaldehyde, despite a lower activity. The catalytic property correlated to the size-dependent oxidation state of the Pt nanoparticles. Transmission electron microscopy (TEM) imaging revealed the well-defined lattice structures of Pt metal for the 2, 4, and 6 nm nanoparticles, while the 1 nm nanoparticles appeared to be quasicrystalline. X-

Received: April 30, 2013
Revised: May 18, 2013
Published: May 23, 2013

ray photoelectron spectroscopy (XPS) suggested that the 2, 4, and 6 nm Pt nanoparticles were largely metallic, while the 1 nm Pt nanoparticles were predominantly oxidized. This result was further confirmed by a diffuse reflectance infrared Fourier transform spectroscopy (DRIFTS) study of CO adsorbed on the nanoparticles.

Pt nanoparticles with various sizes were synthesized by solution phase reactions with polyvinylpyrrolidone (PVP) as the capping agent (see Supporting Information for details). Low-magnification TEM images of the resulting nanoparticles are shown in Figure 1a–d. Photoreduction of H_2PtCl_6 in aqueous solution at room temperature produced Pt nanoparticles with an average diameter of ~1 nm (Figure 1a). NaOH-assisted reduction of H_2PtCl_6 in ethylene glycol at 160 °C afforded Pt nanoparticles with an average size of ~2 nm (Figure 1b). The ~4 nm Pt nanoparticles were synthesized by reducing H_2PtCl_6 in ethylene glycol at 160 °C (Figure 1c). Reduction of Pt(II) acetylacetonate in ethylene glycol at 200 °C was used to prepare ~6 nm sized Pt nanoparticles (Figure 1d). Size distributions of the Pt nanoparticles are shown in Figure S1.

Figure 1e–h shows high-resolution TEM images of the Pt nanoparticles. Clear lattice fringes corresponding to the (111) or (200) facets of metallic Pt were observed for the 2, 4, and 6 nm nanoparticles (Figure 1f–h). However, the 1 nm nanoparticles exhibited poorly defined lattice fringes (Figure 1e), suggesting an aggregate of Pt atoms rather than a crystalline Pt nanoparticle. In a previous study of Pt clusters inside a dendrimer, a similar "crystalline-to-disordered" transition was also observed in the size range between 1.5 and 2 nm.[18]

XPS measurements were carried out for the synthesized Pt nanoparticles to understand the chemical states of the surface atoms. For 2, 4, and 6 nm nanoparticles, the Pt $4f_{7/2}$ and $4f_{5/2}$ peaks appeared at 71.2 and 74.5 eV, respectively (Figure 2a), consistent with the previous results of metallic Pt nanoparticles capped with PVP.[19] In contrast, the Pt $4f_{7/2}$ and $4f_{5/2}$ peaks of the 1 nm nanoparticles shifted to higher binding energies of

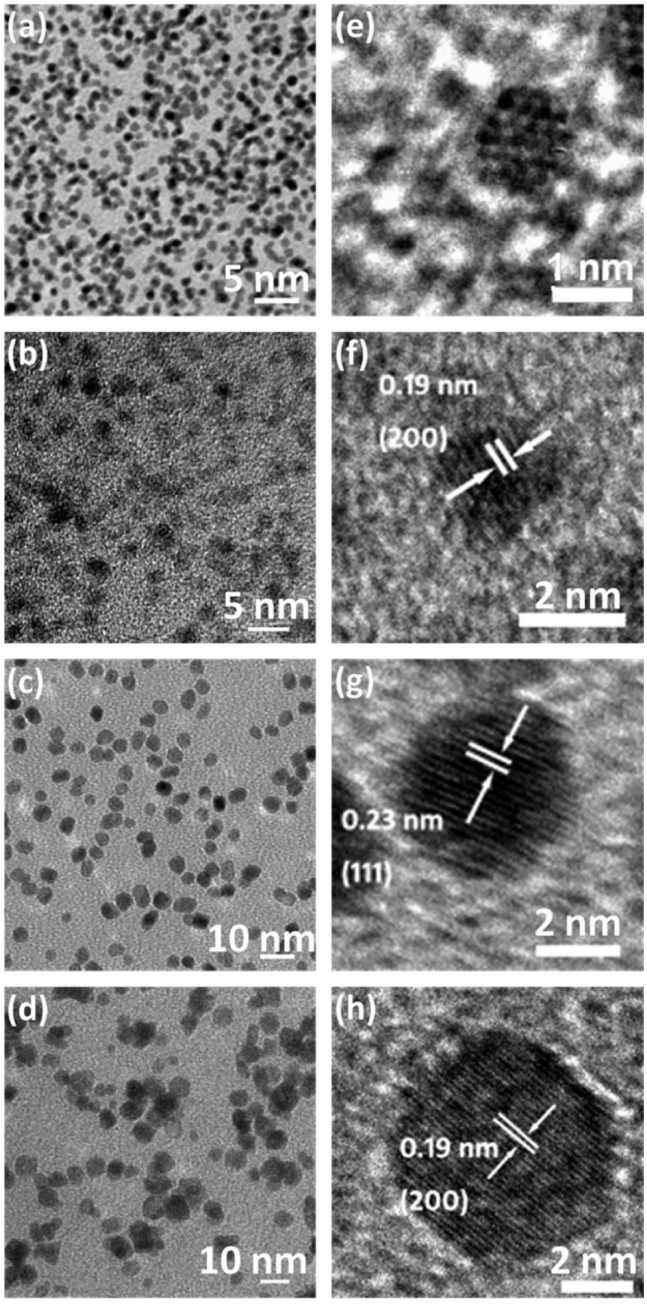

Figure 1. TEM characterization of Pt nanoparticles with various sizes. Low-resolution TEM images of Pt nanoparticles in average sizes of (a) 1 nm, (b) 2 nm, (c) 4 nm, and (d) 6 nm. High-resolution TEM images of Pt nanoparticles in average sizes of (e) 1 nm, (f) 2 nm, (g) 4 nm, and (h) 6 nm.

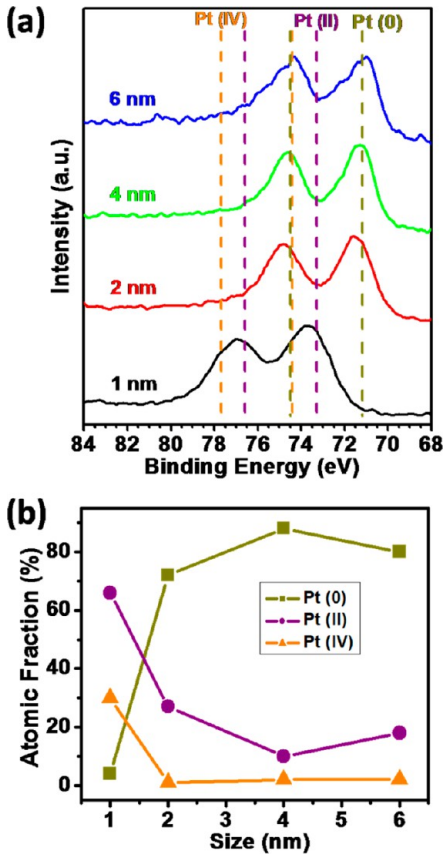

Figure 2. XPS measurements of Pt nanoparticles with various sizes. (a) Pt 4f core level spectra of Pt nanoparticles. The dark yellow, purple, and orange dashed lines mark the binding energy positions of Pt(0), Pt(II), and Pt(IV), respectively. (b) Oxidation state distribution of Pt as estimated from deconvolution of Pt 4f XPS peaks.

dx.doi.org/10.1021/nl401568x | Nano Lett. 2013, 13, 2976–2979

73.6 and 76.9 eV, respectively (Figure 2a). The binding energy shift of +2.4 eV indicated oxidation of Pt atoms. Fitting of the XPS spectra (Figure S2) yielded relative atomic fractions of Pt(0), Pt(II), and Pt(IV) on the surfaces of the nanoparticles. While the 2, 4, and 6 nm Pt nanoparticles were largely metallic with ~72−88% of the atoms in the Pt(0) state, ~96% of the Pt in the 1 nm nanoparticles was in oxidized states (Figure 2b). Considering the probing depth of ~1.6 nm for the Pt 4f region under the incident X-ray photon energy of 1487 eV used in this work, it was quite likely that almost the entire 1 nm nanoparticle was oxidized, which agreed with the structure observed with TEM. Other studies have also observed dominant oxidized Pt in 0.8−1.5 nm Pt nanoparticles synthesized by different methods.[20,21]

The surface structures of the Pt nanoparticles were further probed with DRIFTS using adsorbed CO molecules.[22−25] The stretching vibration mode of gas-phase CO molecules shows a frequency of ~2143 cm^{-1}. The vibrational frequency shifts to lower wavenumbers for CO adsorbed on Pt surface, due to electron backdonation from the Pt atoms to the π^*-orbitals of the CO molecules. The shift in the vibrational frequency is thus a useful indicator of the oxidation states of the Pt atoms.[22−25] Before the measurement, the Pt nanoparticles with various sizes were deposited on Si substrates and treated in CO atmosphere under ambient conditions for more than 12 h to achieve full adsorption of CO on the Pt surface. The 4 and 6 nm nanoparticle samples exhibited absorption peaks at 2053 and 2048 cm^{-1}, respectively (Figure 3), corresponding to the

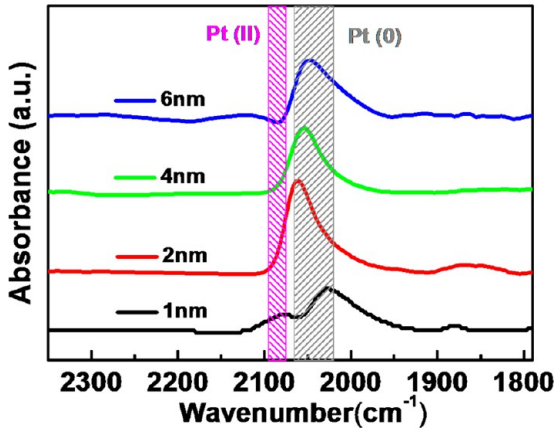

Figure 3. DRIFTS spectra of CO molecules adsorbed on Pt nanoparticles with various sizes. The gray and magenta shaded areas mark the approximate stretching frequency ranges of CO adsorbed on Pt(0) and Pt(II), respectively.

stretching vibration of linearly adsorbed CO molecules on metallic Pt(0) surface. The vibrational frequency slightly shifted to 2061 cm^{-1} for the 2 nm Pt nanoparticle sample (Figure 3). This shift was likely due to partial oxidation of the surface atoms (Figure 2b) and weaker electron backdonation. In contrast, the vibration frequency of the CO molecules adsorbed on the 1 nm sized Pt nanoparticles shifted to 2078 cm^{-1} (Figure 3). The location of this feature indicated the presence of CO molecules adsorbed on oxidized Pt species on the surface of the 1 nm nanoparticles. Another peak at 2026 cm^{-1} was attributed to stretching of CO adsorbed on metallic Pt atoms that were exposed by reduction of the oxidized Pt species during CO treatment.

The Pt nanoparticles were drop-casted onto Si pieces for catalytic measurements for methanol oxidation. The tests were performed in a batch reactor equipped with a boron nitride substrate heater and a metal bellows recirculation pump for gas mixing. The reactor was filled with 10 Torr of methanol, 50 Torr of oxygen (methanol/oxygen = 1:5), and 710 Torr of helium at a temperature of 60 °C. Reaction rates were measured under differential conditions using total conversions below 10%. Formaldehyde and CO_2 were detected by gas chromatography with a thermal conductivity detector.

Formaldehyde and CO_2 were produced simultaneously over the Pt nanoparticle catalysts (Figure 4a). Pt nanoparticle

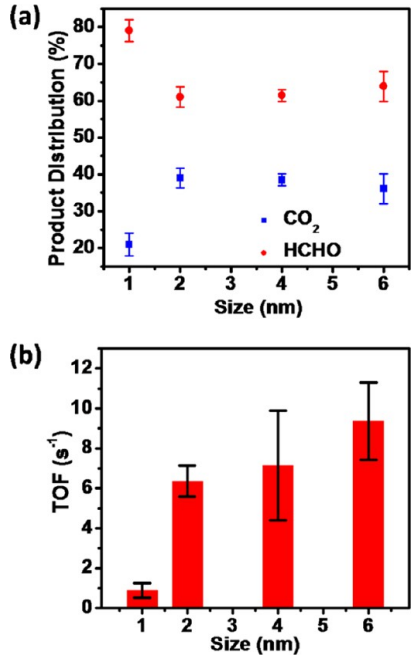

Figure 4. Catalytic performance of Pt nanoparticles with various sizes in methanol oxidation. (a) Product distribution of methanol oxidation reactions catalyzed by Pt nanoparticles with various sizes. (b) Measured TOF of Pt nanoparticles with various sizes for methanol oxidation.

catalysts with average sizes of 2, 4, and 6 nm formed both products with a similar catalytic selectivity of ~3:2 (formaldehyde/CO_2). In comparison, the 1 nm Pt nanoparticle catalysts formed formaldehyde and CO_2 with a product ratio of ~4:1 (Figure 4a). The 1 nm Pt catalysts also exhibited a different net activity (i.e., turnover frequency (TOF)) in comparison to the larger nanoparticles. TOF was derived for each catalyst using a structurally insensitive reaction to probe the number of active sites. Previously, the rate of ethylene hydrogenation on Pt surfaces of different Miller indices and nanoparticle sizes was found to be structurally insensitive.[2,3] We estimated the TOF for methanol oxidation on the Pt nanoparticle catalysts using a reaction rate of 11.7 molecule-$s{\cdot}site^{-1}{\cdot}s^{-1}$ for ethylene hydrogenation on Pt surface at 25 °C as performed previously for other reactions on Pt.[5,11,26] The 1 nm Pt nanoparticles showed a TOF of ~0.9 $molecules{\cdot}site^{-1}{\cdot}s^{-1}$, ~7−11 times lower than the other catalysts with larger particle sizes (Figure 4b).

In light of a previous study that found oxygen dependence in catalytic methanol oxidation over a nanoporous Au catalyst,[27] we performed catalysis measurements with 10 Torr of

dx.doi.org/10.1021/nl401568x | Nano Lett. 2013, 13, 2976−2979

methanol and 5 Torr of oxygen (methanol/oxygen = 2:1) in a helium background (755 Torr) at 60 °C over the 2, 4, and 6 nm Pt nanoparticle catalysts. Although the methanol/oxygen ratio was stoichiometric for formaldehyde production, the product distribution remained unchanged in comparison to a reaction performed with a methanol/oxygen ratio of 1:5. The catalytic selectivity was not affected by the partial pressure of oxygen. Such a negligible response to oxygen was different than observed in the previous study with a nanoporous Au catalyst.[27] Under a stoichiometric gas composition (methanol/oxygen = 2:1), methanol was oxidized to form methyl formate, while the full oxidation product (CO_2) was generated with an increased partial pressure of oxygen.[27] We further tested our Pt nanoparticle catalysts with 10 Torr of methanol in a helium background (no oxygen). No turnover of methanol was detected, which excluded the possibility of formaldehyde formation via the route of methanol dehydrogenation.

Combining the results of catalytic study with those of microscopy and spectroscopy measurements, we believe that the size effect observed over Pt nanoparticles with average sizes of 1, 2, 4, and 6 nm for gas-phase methanol oxidation reaction is more likely due to the change of nanoparticle structure and Pt oxidation state than the percentage of step/edge sites on the surface. When the size of Pt nanoparticles was reduced to 1 nm, the Pt atoms became oxidized rather than metallic and the nanoparticle structure turned from crystalline to quasicrystalline. Such changes could lead to significant alterations in catalytic behavior and are critically important to understanding the size effect of metal nanoparticles in catalysis. In this work, two interpretations may account for the different catalytic behaviors observed with the Pt nanoparticle catalysts of different sizes. The binding of methanol intermediates on the oxidized Pt surface of the 1 nm nanoparticles could be weaker in comparison with the metallic surface of the larger nanoparticles. Weakened adsorption strength of the intermediates will shorten their residence time on the catalyst surface and subsequently lead to lower methanol oxidation rate as well as lower selectivity toward full oxidation of methanol to CO_2. Another interpretation of the observed size effect relates to the lower reactivity of the oxygen on the oxidized surface of the 1 nm nanoparticles compared to the chemisorbed oxygen on the metallic surface of the larger nanoparticles.[20] However, the detailed reaction mechanism still remains to be elucidated by future study.

In summary, we synthesized Pt nanoparticles with various sizes for selective oxidation of methanol in the gas phase. High selectivity toward partial oxidation to formaldehyde as well as a lower total TOF were observed when the size of Pt nanoparticles was reduced to 1 nm, due to change of the structure of the nanoparticles when the Pt atoms became oxidized. This work suggests the possibility of tuning particle size of Pt nanoparticles for selective catalysis.

■ ASSOCIATED CONTENT

Supporting Information

Experimental details of Pt nanoparticle synthesis, TEM, XPS, DRIFTS, and catalytic study. This material is available free of charge via the Internet at http://pubs.acs.org.

■ AUTHOR INFORMATION

Corresponding Author

*E-mail: somorjai@berkeley.edu.

Notes

The authors declare no competing financial interest.

■ ACKNOWLEDGMENTS

This work is supported by the Director, Office of Science, Office of Basic Energy Sciences of the U.S. Department of Energy under Contract No. DE-AC02-05CH11231. H.W. acknowledges support from the Philomathia Postdoctoral Fellowship. Y.W. appreciates support from Basic Research Program of Young Scientists by National Natural Science Foundation of China and Chinese University of Hong Kong.

■ REFERENCES

(1) Somorjai, G. A.; Li, Y. *Introduction to surface chemistry and catalysis*; Wiley: New York, 2010.
(2) Rioux, R. M.; Song, H.; Hoefelmeyer, J. D.; Yang, P.; Somorjai, G. A. *J. Phys. Chem. B* **2005**, *109*, 2192.
(3) Tsung, C.-K.; Kuhn, J. N.; Huang, W.; Aliaga, C.; Hung, L.-I.; Somorjai, G. A.; Yang, P. *J. Am. Chem. Soc.* **2009**, *131*, 5816.
(4) Alayoglu, S.; Pushkarev, V. V.; Musselwhite, N.; An, K.; Beaumont, S. K.; Somorjai, G. A. *Top. Catal.* **2012**, *55*, 723.
(5) Alayoglu, S.; Aliaga, C.; Sprung, C.; Somorjai, G. *Catal. Lett.* **2011**, *141*, 914.
(6) Grass, M. E.; Rioux, R. M.; Somorjai, G. A. *Catal. Lett.* **2009**, *128*, 1.
(7) Rioux, R.; Hsu, B.; Grass, M.; Song, H.; Somorjai, G. A. *Catal. Lett.* **2008**, *126*, 10.
(8) Kuhn, J. N.; Huang, W.; Tsung, C.-K.; Zhang, Y.; Somorjai, G. A. *J. Am. Chem. Soc.* **2008**, *130*, 14026.
(9) Shao, M.; Peles, A.; Shoemaker, K. *Nano Lett.* **2011**, *11*, 3714.
(10) An, K.; Somorjai, G. A. *ChemCatChem* **2012**, *4*, 1512.
(11) Pushkarev, V. V.; An, K.; Alayoglu, S.; Beaumont, S. K.; Somorjai, G. A. *J. Catal.* **2012**, *292*, 64.
(12) Michalak, W. D.; Krier, J. M.; Komvopoulos, K.; Somorjai, G. A. *J. Phys. Chem. C* **2013**, *117*, 1809.
(13) Tritsaris, G.; Greeley, J.; Rossmeisl, J.; Nørskov, J. K. *Catal. Lett.* **2011**, *141*, 909.
(14) Li, L.; Larsen, A. H.; Romero, N. A.; Morozov, V.; Glinsvad, C.; Abild-Pedersen, F.; Greeley, J. P.; Jacobsen, K. W.; Norskov, J. K. *J. Phys. Chem. Lett.* **2012**, *4*, 222.
(15) Kleis, J.; Greeley, J.; Romero, N.; Morozov, V.; Falsig, H.; Larsen, A. H.; Lu, J.; Mortensen, J. J.; Dułak, M.; Thygesen, K. S. *Catal. Lett.* **2011**, *141*, 1067.
(16) Liu, H.; Song, C.; Zhang, L.; Zhang, J.; Wang, H.; Wilkinson, D. P. *J. Power Sources* **2006**, *155*, 95.
(17) Vinod, C. P.; Wilson, K.; Lee, A. F. *J. Chem. Technol. Biotechnol.* **2011**, *86*, 161.
(18) Borodko, Y.; Ercius, P.; Pushkarev, V.; Thompson, C.; Somorjai, G. *J. Phys. Chem. Lett.* **2012**, *3*, 236.
(19) Sevilla, M.; Sanchís, C.; Valdés-Solís, T.; Morallón, E.; Fuertes, A. *Electrochim. Acta* **2009**, *54*, 2234.
(20) Butcher, D. R.; Grass, M. E.; Zeng, Z.; Aksoy, F.; Bluhm, H.; Li, W.-X.; Mun, B. S.; Somorjai, G. A.; Liu, Z. *J. Am. Chem. Soc.* **2011**, *133*, 20319.
(21) Huang, W.; Kuhn, J. N.; Tsung, C.-K.; Zhang, Y.; Habas, S. E.; Yang, P.; Somorjai, G. A. *Nano Lett.* **2008**, *8*, 2027.
(22) Kappers, M.; Van der Maas, J. *Catal. Lett.* **1991**, *10*, 365.
(23) Bazin, P.; Saur, O.; Lavalley, J.; Daturi, M.; Blanchard, G. *Phys. Chem. Chem. Phys.* **2005**, *7*, 187.
(24) Einaga, H.; Harada, M. *Langmuir* **2005**, *21*, 2578.
(25) Qiao, B.; Wang, A.; Yang, X.; Allard, L. F.; Jiang, Z.; Cui, Y.; Liu, J.; Li, J.; Zhang, T. *Nat. Chem.* **2011**, *3*, 634.
(26) Baker, L. R.; Kennedy, G.; Van Spronsen, M.; Hervier, A.; Cai, X.; Chen, S.; Wang, L.-W.; Somorjai, G. A. *J. Am. Chem. Soc.* **2012**, *134*, 14208.
(27) Wittstock, A.; Zielasek, V.; Biener, J.; Friend, C.; Bäumer, M. *Science* **2010**, *327*, 319.